Synthesis, Characterization, and Aggregation Behavior of Block Copolymers Bearing Blocks of Lipid−Mimetic Aliphatic Double Chain Units

S. Rangelov,*,†,‡ M. Almgren,† Ch. Tsvetanov,‡ and K. Edwards†

Department of Physical Chemistry, University of Uppsala, Box 532, 751 21 Uppsala, Sweden, and Institute of Polymers, Bulgarian Academy of Sciences, 1113 Sofia, Bulgaria

Received December 27, 2001; Revised Manuscript Received March 22, 2002

ABSTRACT: A number of diblock and triblock copolymers of ethylene oxide and 1,3-didodecyloxy-2-glycidyl-glycerol (DDGG), an epoxide monomer bearing a lipid−mimetic anchor, were synthesized via anionic polymerization. The copolymers were characterized by ^{1}H nuclear magnetic resonance spectroscopy and gel permeation chromatography. Their self-association in aqueous environment was studied by simultaneous static and dynamic light scattering, and the particles were visualized by means of cryogenic transmission electron microscopy. The weight-average molecular weights, the radii of gyration, the second virial coefficients, the diffusion coefficients, and the hydrodynamic radii of the particles were determined. The particles were of nanodimensions with weight-average molecular weights up to tens of millions and consisted of hydrophobic poly(DDGG) and hydrophilic PEG chains in the core and corona, respectively. The results indicate formation of PEG−water domains randomly distributed in the cores. Dynamic light scattering of selected copolymers carried out in extended temperature and concentration intervals revealed a formation of dense particles. The density of the particles was found to increase with a temperature increase.

Introduction

Considerable research efforts have been devoted to development of vesicles (liposomes) for the delivery of drugs. In the past two decades, vesicle compositions which prolong vesicle circulation time in the blood-stream were discovered.[1−12] The basic strategy is to create a steric repulsive barrier around the liposome that decreases interactions with various blood proteins. The formation of such sterically stabilized liposomes is usually achieved by utilization of derivatives of dialkyl-substituted glycerols with covalently attached poly-(ethylene glycol) (PEG), referred to as PEG lipids.[13−21] The actual mechanism by which the stabilization occurs involves intercalation of the hydrophobic double chain moiety in the lipid membrane while the PEG chains grafted on the membrane form a dense hydrophilic layer around it. The molecules of the PEG lipids, however, contain only one lipid−mimetic residue. It has been assumed earlier[22] that copolymers containing short blocks of repeating lipid−mimetic monomer units would provide a better anchorage of the copolymer molecule in the bilayer membrane. To prepare such copolymers, however, monomers bearing both a polymerizable group and a lipid−mimetic moiety are needed. In previous papers,[22,23] the synthesis and polymerizability of such epoxide monomers, 1,3-didodecyloxy-2-glycidylglycerol (hereinafter DDGG) and glycidyldidodecylamine, are reported. The chemical structure of DDGG is presented in Figure 1a. It was shown that the monomers can homopolymerize and copolymerize with ethylene oxide (EO) in the presence of an anionic initiator. Homopolymers as well as diblock copolymers denoted $(EO)_{114}$-$(DDGG)_2$ and $(EO)_{114}(DDGG)_{32}$ were prepared, and a preliminary investigation of their properties has been presented.[22]

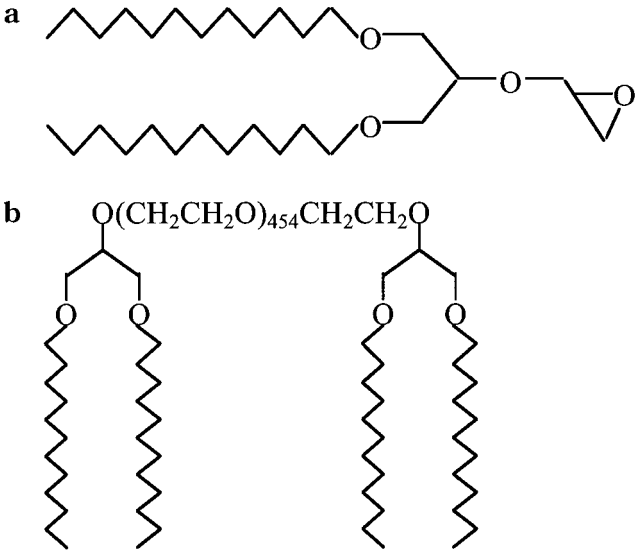

Figure 1. Chemical structure of DDGG (a) and $(didodecyl)_2$-PEG20K (b).

The present paper continues the earlier research. It deals with the synthesis and characterization of various diblock and triblock copolymers of DDGG and EO. We focus our attention on the properties of the above copolymers in aqueous media. The associative behavior is studied by a combination of static and dynamic light scattering as well as cryogenic transmission electron microscopy. Using the same techniques, aqueous solutions of copolymers that have been synthesized earlier, $(EO)_{114}(DDGG)_2$[22] and aliphatic double chain end-capped PEG 20000 [hereinafter $(didodecyl)_2$PEG20K],[24] are investigated and the results reported. The chemical structure of the latter is presented in Figure 1b.

The novel polyethers investigated in the present study may find other uses than the steric stabilization of

† University of Uppsala.
‡ Bulgarian Academy of Sciences.

10.1021/ma012246+ CCC: $22.00
Published on Web 05/03/2002

Table 1. Degrees of Polymerization and Polydispersity of the Starting PEG and PEG Monomethyl Ether Precursors

abbreviation	deg of polymerization	M_w/M_n (GPC)
PEG 5000 MME	114	1.07
PEG 10 000 MME	227	1.04
PEG 6000	136	1.05
PEG 10 000	227	1.04
PEG 20 000	454	1.05

liposomes. Their composition, in particular the unique structure of the hydrophobic monomer unit, suggests that they have potential applications in a variety of other interesting, attractive, and important fields such as drug delivery, solubilization of active products, lipid emulsion stabilization, surface modification, formation of self-assembled structures, thickening, etc.

Experimental Section

Materials. All solvents and reagents were supplied by Fluka or Aldrich. The solvents were purified by standard methods whereas the reagents were used as received. Poly(ethylene glycol) monomethyl ethers (PEG MME) of weight-average molecular weights 5000 and 10 000 and PEGs of weight-average molecular weights 6000, 10 000, and 20 000 (see Table 1 for the degrees of polymerization and polydispersity) were dried by azeotropic distillation from toluene. DDGG, $(EO)_{114}(DDGG)_2$, and $(didodecyl)_2PEG20K$ were prepared according to procedures described elsewhere.[22,24]

Synthesis of Diblock Copolymers. 2.95 g (5.90×10^{-4} mol) of PEG 5000 MME previously metaled by potassium naphthalide was dissolved in 25 mL of toluene and placed in a 50 mL three-necked flask fitted with a nitrogen inlet, a reflux condenser, and a rubber septum. 2.03 g (4.19×10^{-3} mol) of DDGG dissolved in 5 mL of toluene was injected via a syringe. The reaction was carried out at reflux for 48 h. Then toluene was removed under reduced pressure, and the residue was dissolved in methylene chloride. The copolymer was isolated by precipitation in hexane and washed with portions of 30 mL of hexane until no more hexane-soluble fraction was extracted. 3.85 g of a white solid was isolated and dried in a vacuum up to a constant weight. No signals of hydroxyl groups were detected in the ^{1}H NMR spectrum of the product in DMSO, suggesting that all hydroxyl groups had reacted. The syntheses of the other diblock copolymers were carried out in analogy to this procedure.

Synthesis of Triblock Copolymers. 3.25 g (3.25×10^{-4} mol) of PEG 10 000 previously metaled by potassium naphthalide was dissolved in 25 mL of toluene and placed in a 50 mL three-necked flask fitted with a nitrogen inlet, a reflux condenser, and a rubber septum. 1.57 g (3.25×10^{-3} mol) of DDGG dissolved in 5 mL of toluene was injected via a syringe. The reaction was carried out at reflux for 48 h. Then toluene was removed under reduced pressure, and the residue was dissolved in methylene chloride. The copolymer was isolated by precipitation in hexane and washed with portions of 30 mL of hexane until no more hexane-soluble fraction was extracted. 3.30 g of a white solid was isolated and dried in a vacuum up to a constant weight. No signals of hydroxyl groups were detected in the ^{1}H NMR spectrum of the product in DMSO, suggesting that all hydroxyl groups had reacted. The syntheses of the other triblock copolymers were carried out in analogy to this procedure.

Methods. *Nuclear Magnetic Resonance (NMR).* ^{1}H NMR spectra were recorded at 250 MHz on a Bruker 250 spectrometer. The samples were prepared as solutions in $CDCl_3$ or DMSO. The chemical shifts are given in ppm from tetramethylsilane. All spectra were recorded at 25 °C.

Gel Permeation Chromatography (GPC). The GPC system (Waters) consisted of four styragel columns with nominal pore sizes of 100, 500, 500, and 1000 Å, eluted with tetrahydrofuran at 40 °C. The flow rate of the eluent was 1 mL/min. Samples were prepared as solutions in tetrahydrofuran. Elution volumes were referenced to toluene as internal standard. Calibration was done with PEG standards, and derived weight-average molar masses and degrees of polymerization were determined as if samples were PEG.

Light Scattering. The light scattering setup consists, as described previously,[25] of a 488 nm Ar ion laser and the detector optics with an ITT FW 130 photomultiplier and ALV-PM-PD amplifier−discriminator connected to an ALV-5000 autocorrelator built into a computer. The cylindrical scattering cells were sealed and then immersed in a large-diameter thermostated bath containing the index matching fluid decalin. Measurements were made at different angles in the range 50−130° and at different concentrations and temperatures. Information on the molecular weight, the radius of gyration, and the second virial coefficient was obtained from the static light scattering data using the Zimm plot method. The angular dependence of the reduced scattered intensity, Kc/R_Θ, of a number of copolymer solutions was measured in the simultaneous static and dynamic experiments. Here $K = (4\pi^2 n^2/N_A\lambda^4)(dn/dc)^2$, N_A is Avogadro's constant, and λ is the wavelength of the light in a vacuum. The refractive index increment (dn/dc) was measured in a differential refractometer with Rayleigh optics. For the present systems, $dn/dc = 0.134$ mL g^{-1} at the wavelength used and 25 °C. The Rayleigh ratio was determined as $R_\Theta = [(I - I_0)/I_{ref}]R_{ref}(n/n_{ref})^2$. Here $n = 1.33$ is the solvent refractive index and n_{ref} that of toluene. I is the measured total time-average scattered intensity, I_0 that of the solvent, water, and I_{ref} that of toluene. Toluene was used as the reference scatterer ($R_{ref} = 4.0 \times 10^{-3}$ m^{-1} at $\lambda = 488$ nm[25]). The reduced scattered intensity was either linearly dependent on $\sin^2(\Theta/2)$ or just slightly curved at higher angles, indicating that the angle range was appropriately chosen. Here Θ is the scattering angle.

Analysis of the dynamic data was performed by fitting the experimentally measured $g_2(t)$, the normalized intensity autocorrelation function, which is related to the electrical field correlation function $g_1(t)$ by the Siegert relationship:[26]

$$g_2(t) - 1 = \beta|g_1(t)|^2 \tag{1}$$

where β is a factor accounting for deviation from ideal correlation. For polydisperse samples, $g_1(t)$ can be written as the inverse Laplace transform (ILT) of the relaxation time distribution, $\tau A(\tau)$:

$$g_1(t) = \int \tau A(\tau) \exp(-t/\tau)\, d \ln \tau \tag{2}$$

where t is the lag time. The relaxation time distribution, $\tau A(\tau)$, is obtained by performing ILT using the constrained regularization algorithm REPES,[27] which minimizes the sum of the squared differences between the experimental and calculated $g_2(t)$. A mean diffusion coefficient D is calculated from the second moment of each peak as $D = \Gamma/q^2$, where q is the magnitude of the scattering vector $q = (4\pi n/\lambda)\sin(\Theta/2)$ and $\Gamma = 1/\tau$ is the relaxation rate of each mode. With some exceptions the relaxation time distributions were monomodal. Here Θ is the scattering angle, n the refractive index of the medium, and λ the wavelength of the light in a vacuum.

Within the dilute regime, D varies linearly with the concentration according to

$$D = D_0(1 + k_D C + ...) \tag{3}$$

where D_0 is the diffusion coefficient at infinite dilution and k_D is the hydrodynamic "virial" coefficient related to the second virial coefficient A_2 by

$$k_D = 2A_2M - k_f - 2\nu_2 \tag{4}$$

Here M is the molar mass, k_f defines the concentration dependence of the friction coefficient in $f = f_0(1 + k_f C + ...)$, and ν_2 is the partial specific volume.

The Stokes−Einstein equation relates D_0 to the hydrodynamic radius (R_h):

$$R_h = kT/(6\pi\eta D_0) \quad (5)$$

kT is the thermal energy factor, and η is the temperature-dependent viscosity of water.

Cryogenic Transmission Electron Microscopy (Cryo-TEM). Transmission electron microscopy observations were conducted on a Zeiss EM 902 A instrument operating at 80 kV. The procedure for the sample preparation is described in the following. A drop of the dispersion is deposited on an electron microscopy copper grid coated by a perforated polymer film. The excess of the liquid is blotted by a filter paper, leaving a thin film of the dispersion on the grid. The above operations are performed in a special chamber where the environmental conditions (constant temperature and high humidity) are under strict control. The film on the grid is vitrified by plunging the grid into liquid ethane held at temperature below 100 K. During the rapid cooling of the aqueous film vitreous ice is formed instead of crystalline ice that is formed when the water solution is cooled slowly. The vitrified sample is then transferred to the microscope for observation. The observation and the transfer are done at temperatures below 100 K.

Results

Block Copolymer Synthesis. In contrast to $(EO)_{114}$-$(DDGG)_2$, which was prepared by sequential anionic polymerization of EO followed by DDGG,[22] the AB diblock copolymers were prepared using PEG 5000 MME and PEG 10 000 MME. An appropriate quantity of DDGG was added to the previously metaled by potassium naphthalide precursors, and the reactions were carried out in toluene at reflux for 48 h. The block structure of the resulting copolymers was proved by GPC. Figure 2a shows the GPC curves of the PEG 5000 MME precursor and the resulting AB diblock copolymer. The copolymer compositions were determined from the ^{1}H NMR spectra from the relative intensities of the resonances of the methylene protons of the PEG moieties at 3.5−3.7 ppm and the methyl protons of the dodecyl chains at 0.8 ppm[22] (Figure 3), assuming the degrees of polymerization of the PEG moieties given in Table 1. The compositions are as follows: $(EO)_{114}$-$(DDGG)_{3.7}$ and $(EO)_{227}(DDGG)_{4.5}$.

Similarly, BAB triblock copolymers, where A and B represent the PEG and the polylipid moieties, respectively, were obtained. Here, PEGs with weight-average molecular weights of 6000, 10 000, and 20 000 were used. The GPC traces for the PEG 10 000 precursor and the resulting triblock copolymer are presented in Figure 2b. The compositions determined from the ^{1}H NMR spectra are the following: $(DDGG)_2(EO)_{136}(DDGG)_2$, $(DDGG)_{2.3}(EO)_{227}(DDGG)_{2.3}$, and $(DDGG)_{3.6}(EO)_{454}$-$(DDGG)_{3.6}$.

Light Scattering Experiments. Static (SLS) and dynamic (DLS) light scattering experiments were performed simultaneously on aqueous dispersions of each AB and BAB block copolymers in a wide concentration range. Other diblock and triblock copolymers, $(EO)_{114}$-$(DDGG)_2$ and $(didodecyl)_2$PEG20K, that have been synthesized earlier[22,24] were also investigated by light scattering.

Generally, the copolymers in aqueous surrounding form spontaneously large aggregates, as revealed by DLS (not shown). The dispersions are not stable and tend to phase-separate. Following extrusion through a 200 nm pore size filter, however, it was possible to obtain dispersions that are stable over a time scale of months (see later in Discussion).

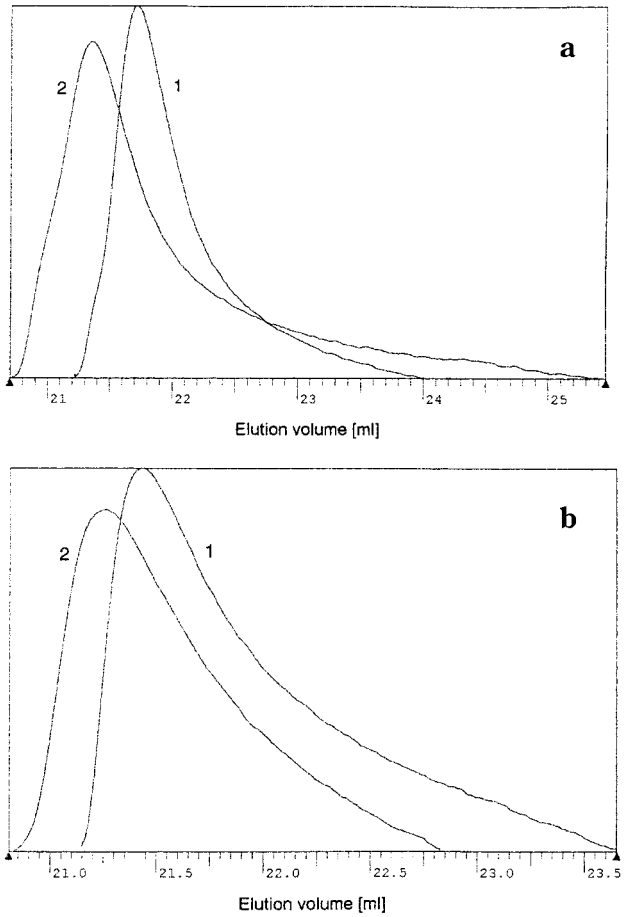

Figure 2. (a) GPC curves of the PEG 5000 MME precursor (curve 1) and the resulting diblock copolymer (curve 2). (b) GPC curves of the PEG 10 000 precursor (curve 1) and the resulting triblock copolymer (curve 2).

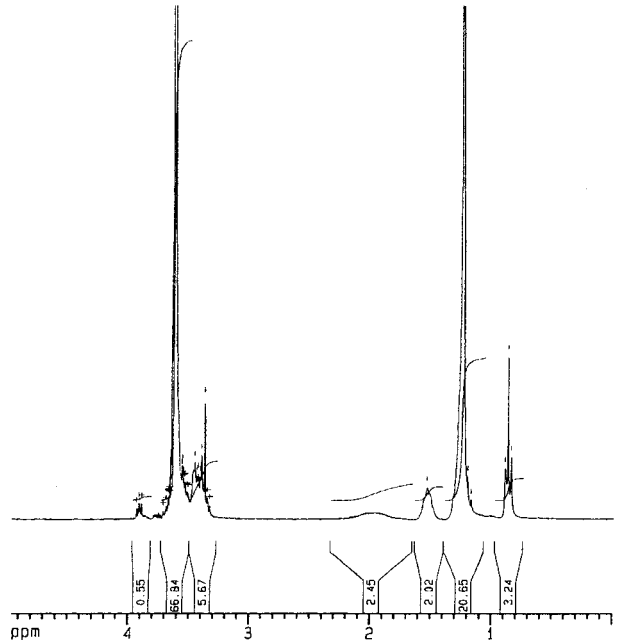

Figure 3. ^{1}H NMR spectrum of $(EO)_{114}(DDGG)_{3.7}$.

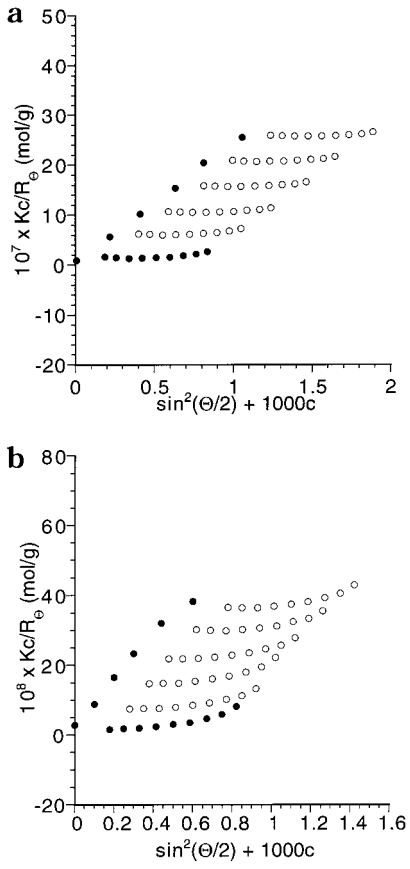

Figure 4. Zimm plots of $(EO)_{114}(DDGG)_{3.7}$ (a) and $(DDGG)_2$-$(EO)_{136}(DDGG)_2$ (b) in water at 25 °C: experimental points (open symbols); extrapolated points to zero concentration and zero scattering angle (filled symbols).

Static Light Scattering Parameters. SLS experiments were carried out at 25 °C in the concentration ranges far below the onset of multiple scattering. It is important to emphasize that at these concentrations the relaxation rate distributions are predominantly monomodal and the relaxation rates practically concentration independent. The concentration ranges varied with the copolymer composition and were typically between 1.0×10^{-4} and 12.0×10^{-4} g/mL. On the other hand, these concentrations are well above the critical aggregation concentrations. The latter for commercial PEG lipids vary depending on the nature of the lipid anchor and the PEG molecular weight and are quite low—some μM.[8,28−32] Since the present copolymers are much more hydrophobic than the commercial PEG lipids, we believe that they exist as unimers only at extreme dilution. The only exception, $(didodecyl)_2$PEG20K, is discussed later.

Weight-average molecular weights, radii of gyration, and second virial coefficients were evaluated from the Zimm plots. Zimm plots for $(EO)_{114}(DDGG)_{3.7}$ and $(DDGG)_2(EO)_{136}(DDGG)_2$, as representative of the diblock and triblock copolymers, respectively, are shown in Figure 4. SLS parameters are collected in Table 2.

The particles were nanoscale in size with weight-average molecular weights ranging from 3.6×10^6 to 40.8×10^6 g/mol. The second virial coefficients were invariably positive, indicating favorable particle/solvent interactions. Furthermore, the aggregation numbers, N_{agg}, were calculated using molecular weight data from Table 2 and the nominal molecular weights of the copolymers. They vary from several hundred to thousands of macromolecules per a particle.

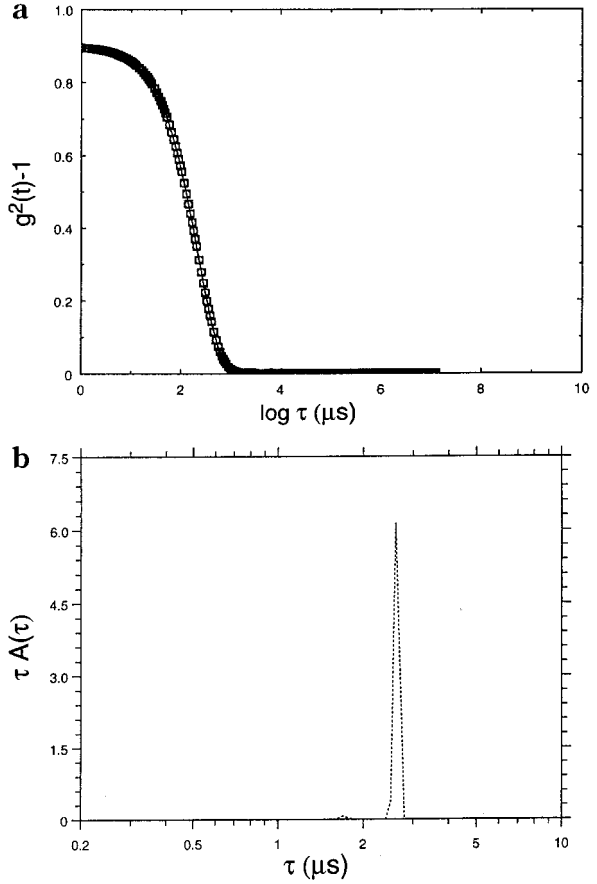

Figure 5. (a) Autocorrelation function for $(DDGG)_2(EO)_{136}$-$(DDGG)_2$ at $c = 0.20 \times 10^{-3}$ g/mL, angle 90°, and temperature 25 °C. (b) Corresponding relaxation time distribution data in (a).

Table 2. Static Light Scattering Characterization Data

formula	$10^{-6}M_w$ (g/mol)	10^4A_2 (mol mL/g^2)	R_g (nm)	N_{agg}
$(EO)_{115}(DDGG)_2$	3.6	1.08	52.5	604
$(EO)_{114}(DDGG)_{3.7}$	6.1	0.266	48.8	896
$(EO)_{227}(DDGG)_{4.5}$	25.6	0.096	86.5	2104
$(DDGG)_2$ $(EO)_{136}(DDGG)_2$	29.0	0.322	81.0	3662
$(DDGG)_{2.3}$ $(EO)_{227}(DDGG)_{2.3}$	40.8	0.289	74.2	3340
$(DDGG)_{3.6}$ $(EO)_{454}(DDGG)_{3.6}$	21.5	0.257	82.0	916
$(didodecyl)_2$ PEG20K	3.9	0.267	93.7	187

Dynamic Parameters. Examples of a correlation function and the corresponding relaxation time distribution function obtained by inverse Laplace transform using REPES algorithm are presented in Figure 5a,b for $(DDGG)_2(EO)_{136}(DDGG)_2$ at $c = 0.20 \times 10^{-3}$ g/mL. Generally, the correlation functions for all copolymers studied were single-exponential and the distributions monomodal. The distributions of $(EO)_{227}(DDGG)_{4.5}$ and $(DDGG)_{2.3}(EO)_{227}(DDGG)_{2.3}$, however, contained a low-amplitude slow mode that varied with the samples, concentration, and angles and accounted for less than 12%. This means that the SLS parameters listed in Table 2 for these two copolymers contained contributions from the slow modes, and the molecular weights and radii of gyration are slightly overestimated, therefore.

The dominant peaks of the copolymers $(EO)_{227}$-$(DDGG)_{4.5}$ and $(DDGG)_{2.3}(EO)_{227}(DDGG)_{2.3}$ as well as the peaks of the rest of the copolymers studied were shown to be diffusive from the linear plots of the

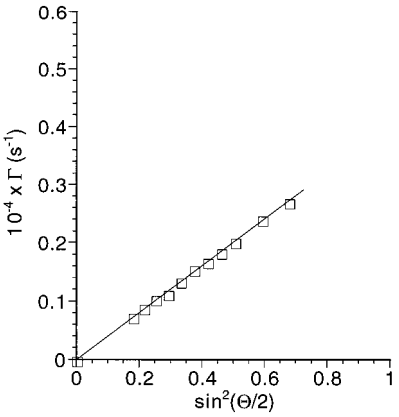

Figure 6. Relaxation rate (Γ) as a function of $\sin^2(\Theta/2)$ for $(DDGG)_{2.3}(EO)_{227}(DDGG)_{2.3}$ at $c = 0.4 \times 10^{-3}$ g/mL and 25 °C.

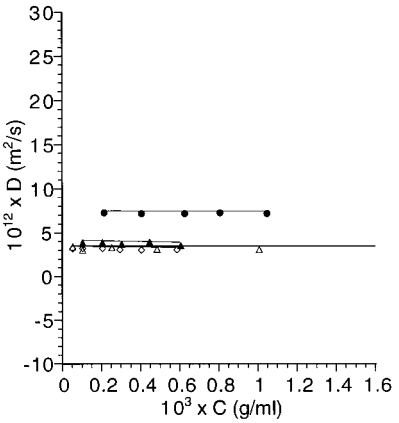

Figure 7. Concentration dependence of diffusion coefficients for $(EO)_{114}(DDGG)_{3.7}$ (filled circles), $(DDGG)_2(EO)_{136}(DDGG)_2$ (filled triangles), $(DDGG)_{3.6}(EO)_{454}(DDGG)_{3.6}$ (open diamonds), and $(didodecyl)_2$PEG20K (open triangles).

Table 3. Dynamic Light Scattering Characterization Data

formula	$10^{12}D$ (m^2/s)	R_h (nm)	R_g/R_h
$(EO)_{115}(DDGG)_2$	7.801	31.4	1.67
$(EO)_{114}(DDGG)_{3.7}$	7.540	32.5	1.50
$(EO)_{227}(DDGG)_{4.5}$	3.810	64.3	1.35
$(DDGG)_2$ $(EO)_{136}(DDGG)_2$	4.205	58.3	1.39
$(DDGG)_{2.3}$ $(EO)_{227}(DDGG)_{2.3}$	3.494	70.1	1.06
$(DDGG)_{3.6}$ $(EO)_{454}(DDGG)_{3.6}$	3.502	70.0	1.17
$(didodecyl)_2$ PEG20K	3.541	69.2	1.35

relaxation rates vs $\sin^2 \Theta/2$ (Figure 6). The diffusion coefficients were determined as slopes of the linear fit. They were then plotted against concentration and extrapolated to zero concentration (Figure 7). The diffusion coefficients showed a weak concentration dependence with the hydrodynamic virial coefficients, k_D, consistently negative (eq 3). This suggests weak attractive interactions between the aggregates in water probably of van der Waals origin. Using the equation of Stokes−Einstein (eq 5), the hydrodynamic radii were calculated. DLS parameters are summarized in Table 3. The R_g/R_h ratio is also shown in Table 3. This ratio gives useful information on the density of the particle structure.[33] R_g/R_h values ranged from 1.06 for $(DDGG)_{2.3}$-$(EO)_{227}(DDGG)_{2.3}$ to 1.67 for $(EO)_{115}(DDGG)_2$ and were thus close to the range 1.1−1.7, typifying starlike polymers or micelles.[34]

In summary, PEG-based block copolymers bearing one or two flanking blocks of repeating lipid anchors form in aqueous media after extrusion through 200 nm filters stable nanosized particles. They presumably consist of lipid−mimetic moieties gathered in hydrophobic domains and flexible PEG chains interacting with water mainly in the outer parts of the particles.

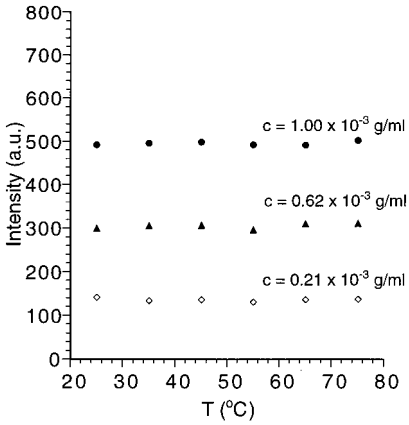

Figure 8. Variation of the scattered light intensity at angle 90° from aqueous dispersions of $(EO)_{114}(DDGG)_{3.7}$ with temperature at three concentrations.

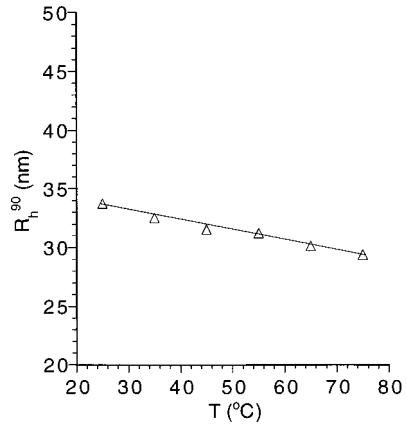

Figure 9. Variation of the hydrodynamic radius measured at angle 90°, R_h^{90}, with temperature for $(EO)_{114}(DDGG)_{3.7}$ at $c = 0.21 \times 10^{-3}$ g/mL.

DLS of Selected Copolymers. To obtain additional information on the hydrodynamic behavior of the copolymers, DLS was carried out in extended temperature and concentration ranges. The measurements were done at various angles in the interval 50−130°. For simplicity, however, only the results obtained at $\Theta = 90°$ are presented. In the following the results for selected copolymers are presented.

$(EO)_{114}(DDGG)_{3.7}$. The variations of the light scattering parameters with temperature were monitored in the concentration range where SLS was carried out (0.21×10^{-3}−1.04×10^{-3} g/mL). The correlation functions were single-exponential and relaxation time distributions monomodal in the whole temperature interval studied (not shown). Figure 8 shows the changes in the scattered light intensity at three concentrations in the range 25−75 °C. As seen, the intensity only varied within the experimental error, and consequently the molecular weights were not affected by the temperature. In contrast, the hydrodynamic radii were found to decrease with increasing temperature (Figure 9), implying formation of more compact particles at elevated temperatures.

$(Didodecyl)_2$PEG20K. Upon decreasing the concentration of $(didodecyl)_2$PEG20K below 0.25×10^{-3} g/mL, a diffusive low-amplitude fast mode appeared. It corresponded to a hydrodynamic radius of 33−36 Å. These

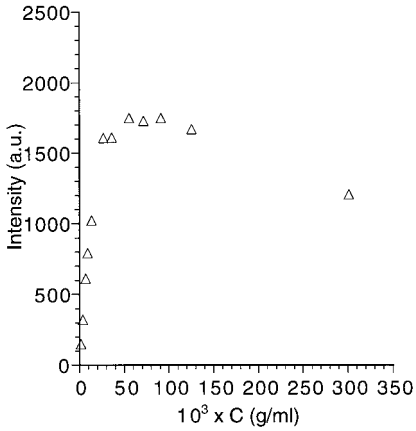

Figure 10. Variation of the scattered light intensity at angle 90° from aqueous solutions of $(didodecyl)_2$PEG20K with concentration at 25 °C.

values are close to the hydrodynamic radius of cyclic molecules of the same molecular weight as $(didodecyl)_2$-PEG20K. A value of 36.9 Å is expected from the empirical relationship (6) of Devanand and Selser,[35] established for unmodified PEG in water

$$R_h = 0.145 M_w^{0.571} \text{ (Å)} \qquad (6)$$

and assuming that the hydrodynamic radius of cyclic molecules is $(0.66)^{1/3}$ of R_h for linear molecules.[36] Indeed, DLS cannot distinguish between the linear and cyclic molecules. In a separate paper,[37] however, the presence of hydrophobic domains at concentrations as low as 3.6×10^{-6} g/mL has been revealed by fluorescence. It is suggested that the hydrophobic domains are formed as a result of intramolecular hydrophobic interactions of the end lipid−mimetic anchors. It is conceivable, therefore, that at concentrations below 0.25×10^{-3} g/mL a fraction of unassociated ring-shaped molecules exists. It completely disappeared upon heating, indicating that all macromolecules were incorporated in the aggregates, and the single-mode behavior was manifested again. With a further dilution and at concentrations as low as 5×10^{-6} g/mL the amplitude of the fast mode did not increase substantially.

Figure 10 shows the variations of the scattered light intensity at $\Theta = 90°$ with $(didodecyl)_2$PEG20K concentration in the range $(3.28-300) \times 10^{-3}$ g/mL. In this concentration range a strong rise in the viscosity was found.[24] The intensity increased linearly up to $c = 26.3 \times 10^{-3}$ g/mL; then, most probably due to multiple scattering, it leveled off and finally dropped down at $c = 300 \times 10^{-3}$ g/mL. The evolution of the relaxation time distributions is shown in Figure 11. As noted above for concentrations lower than 2.5×10^{-3} g/mL, the distributions were generally monomodal and the relaxation rates were concentration-independent. In contrast, at $c > 3.28 \times 10^{-3}$ g/mL the distributions are no longer clearly monomodal. The modes were progressively slowed down with increasing concentration (Figure 11). They were q^2-dependent (not shown) and corresponded to hydrodynamic radii in the 100−600 nm range, reaching thousands of nanometers at $c = 300 \times 10^{-3}$ g/mL.

The temperature dependence of the concentrated solutions of $(didodecyl)_2$PEG20K was investigated as well. Similar to the behavior of $(EO)_{114}(DDGG)_{3.7}$, it was found that in the temperature interval 25−75 °C the scattered light intensity changed within the experimental error, whereas the hydrodynamic radii decreased with approximately 20%. The distributions tended to become monomodal with increasing temperature as demonstrated with the 300×10^{-3} g/mL solution (Figure 11, the upper two traces).

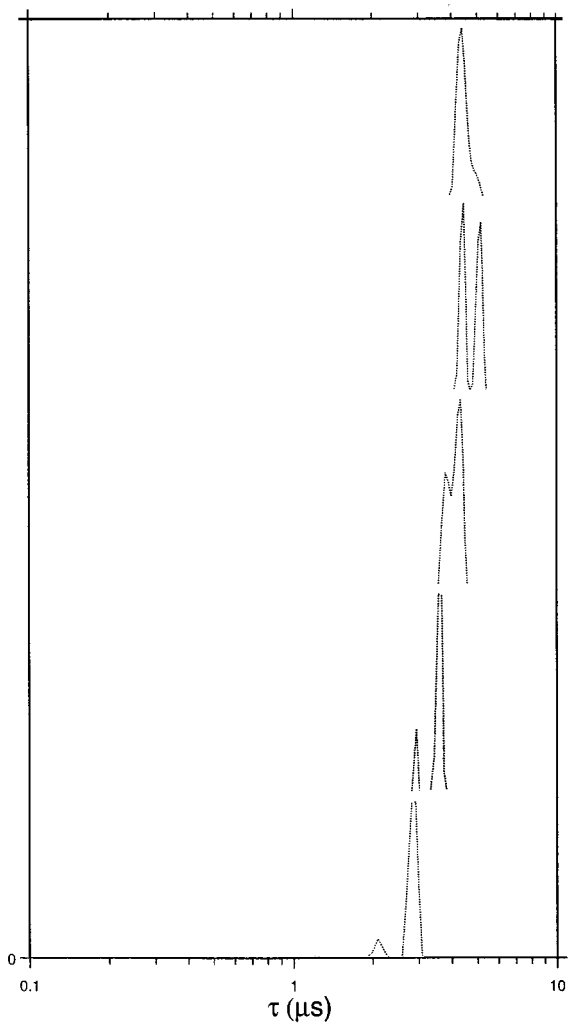

Figure 11. Variation of the relaxation time distributions with $(didodecyl)_2$PEG20K concentration measured at angle 90° and at temperatures 25 and 50 °C. From bottom to top: $c = 3.28 \times 10^{-3}$ g/mL, $t = 25$ °C; $c = 55.4 \times 10^{-3}$ g/mL, $t = 25$ °C; $c = 124.8 \times 10^{-3}$ g/mL, $t = 25$ °C; $c = 300.0 \times 10^{-3}$ g/mL, $t = 25$ °C; $c = 300.0 \times 10^{-3}$ g/mL, $t = 50$ °C.

$(DDGG)_{3.6}(EO)_{454}(DDGG)_{3.6}$. The behavior of $(DDGG)_{3.6}(EO)_{454}(DDGG)_{3.6}$ in the concentration range $(0.10-0.58) \times 10^{-3}$ g/mL was examined at elevated temperatures. Similar to $(EO)_{114}(DDGG)_{3.7}$, the scattered light intensity changed only within the experimental error, and the distribution remained monomodal for the lower concentrations. A low amplitude (up to 7%) slow mode appeared at temperatures higher than 45 °C at the highest concentration studied, $c = 0.58 \times 10^{-3}$ g/mL. This was accompanied by an increase of the scattered light intensity (Figure 12). The results for the diffusion coefficients at three selected copolymer concentrations as well as for the slow mode are expressed as plots of the reduced diffusion coefficient, $D\eta/T$, vs T and are presented in Figure 13. As seen, $D\eta/T$ increases weakly at the copolymer concentrations 0.10×10^{-3} and 0.29×10^{-3} g/mL and for the dominant mode also at 0.58×10^{-3} g/mL. The corresponding hydrodynamic radii were found to decrease with approximately 15%.

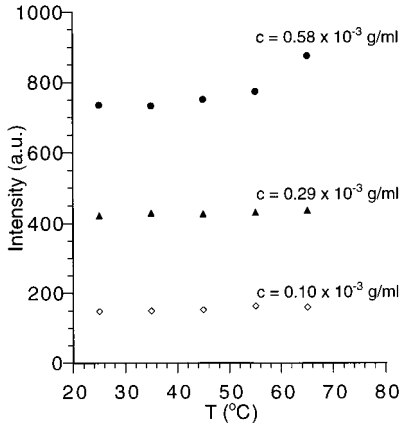

Figure 12. Variation of the scattered light intensity at angle 90° from aqueous dispersions of $(DDGG)_{3.6}(EO)_{454}(DDGG)_{3.6}$ with temperature at three concentrations.

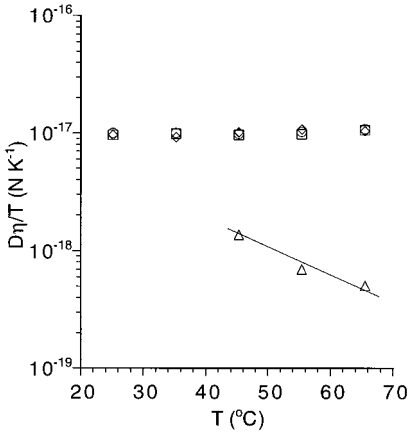

Figure 13. Temperature dependence of the reduced diffusion coefficients of $(DDGG)_{3.6}(EO)_{454}(DDGG)_{3.6}$ at 0.10×10^{-3} g/mL (open circles), 0.29×10^{-3} g/mL (open squares), and 0.58×10^{-3} g/mL (open diamonds) as well of the slow mode at 0.58×10^{-3} g/mL (open triangles).

The quantity $D\eta/T$ for the slow mode at the highest concentration studied and at temperatures higher than 45 °C decreases with increasing temperature. A similar finding has been interpreted earlier by Alami et al.[36] as formation of aggregates due to interactions between the PEG chains which become more attractive upon heating.

Cryo-TEM. The structures represented in Figure 14 are cryo-TEM images of samples of vitrified dispersions of selected copolymers. In the two-dimensional presentation they appear as well-shaped dark circular objects. Since no other but only circular structures were found, it was concluded that the imaged particles were invariably spherical. It is essential to realize that only the cores of the aggregates depicted in Figure 14 are visible. Because of the low contrast between PEG and water, the former are transparent to the electron beam and consequently invisible.

Discussion

PEG-based amphiphilic block copolymers of diblock and triblock chain architecture were synthesized. The hydrophobic sequences of low degrees of polymerization, 2−5, were prepared by anionic polymerization of an epoxide monomer bearing a lipid−mimetic moiety. The latter resembles the lipid anchor of the naturally occurring phospholipids. An important feature of these

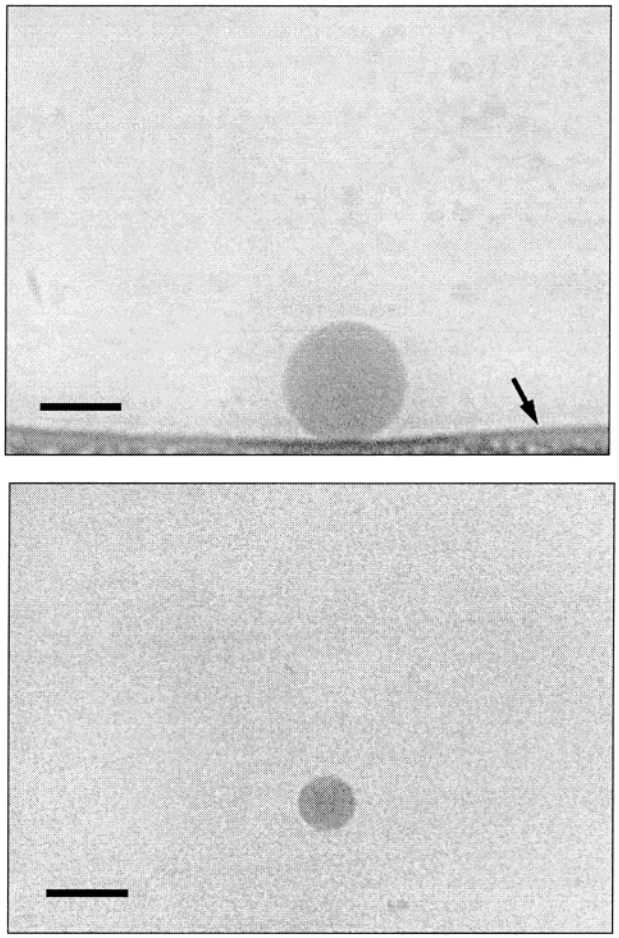

Figure 14. Cryo-TEM micrographs of nanoparticles taken from dispersions of $(DDGG)_{3.6}(EO)_{454}(DDGG)_{3.6}$ (a, top) and $(didodecyl)_2PEG20K$ (b, bottom). The arrow in (a) denotes a perforated polymer film (see Experimental Section). Bar = 100 nm.

novel block copolymers, which makes them different from the commercially available PEG lipids, is that they contain more than one lipid anchor per single polymer chain. Despite the low content of the hydrophobic substituent, the copolymers are not readily soluble in water. By extruding aqueous dispersions, we were able to prepare stable dispersions of uniform nanoparticles. It should be mentioned here that when higher shear forces were applied by using either more concentrated dispersions or more tight filters, the relaxation time distribution as revealed by DLS was no longer monomodal. Similar behavior of polymer species related to our copolymers was observed earlier and interpreted in terms of shear-induced rearrangement of self-assembled structures.[37]

In an aqueous environment the copolymers associate into large multichain aggregates where the poly(DDGG) moieties form the hydrophobic domain, and the PEG chains, in brush or looping conformations for the diblock and triblock copolymers, respectively, are found mainly in the outer parts. The aggregate cores were successfully visualized by cryo-TEM (Figure 14). Probably, the most interesting findings of this study are the dimensions and molecular weights of the particles. They are considered to be quite high for polymers of relatively low both molecular weights and hydrophobic content. Aggregates of similar dimensions and aggregation numbers have been prepared in selective solvents from amphiphilic

polymers of considerably higher molecular weights or/and contents of the insoluble component.[38−44] In our case, the formation of particles of high molecular weights and dimensions could be attributed to the enhanced hydrophobicity achieved by introduction of more than one lipid anchor per polymer chain and, in addition, to some penetration of PEG chains into the aggregate cores (see later in Discussion).

Another aspect of the systems to be considered is the density of the particles as reflected by the ratio R_g/R_h.[33] As noted above, the R_g/R_h values were found to be close to those for micelles.[34] They are somewhat lower for the triblock copolymers, implying that their aggregates are denser than those of the diblock copolymers. It is not fully understood why the triblock architecture favors the formation of more compact particles, though this may be related to the different chain architecture and hence to the different conformations of the PEG chains in the coronae.

An interesting result is also that the particles were found to shrink with increasing temperature. This was registered as a decrease of the hydrodynamic radii of the particles with approximately 12−20% whereas at the same time the scattered light intensity, and consequently the molecular weights, only changed within the experimental error. The concentration ranges at which the LS measurements were carried out were far below the micelle overlap concentrations calculated from R_h assuming face-centered-cubic packing of spheres.[45−47] At these conditions the micelles are isolated and well separated, and therefore interactions between them leading to clustering are unlikely though large clusters were occasionally observed in DLS as a slowly relaxing diffusive component (Figure 13). Since such behavior was manifested only by $(DDGG)_{3.6}(EO)_{454}(DDGG)_{3.6}$, i.e., the copolymer with the highest PEG content, at the highest concentration studied and only at elevated temperatures, it could be attributed to markedly enhanced attractions between the PEG chains upon increasing temperature as a result of their dehydration.[36,48−51] The clustering phenomena at concentrations higher than the overlap concentration were nicely demonstrated with the most hydrophilic member, $(didodecyl)_2$PEG20K (Figure 11). This polymer is readily soluble in water even at concentrations as high as 300×10^{-3} g/mL, and in contrast to the rest of the copolymers no special treatment is needed in order to obtain aqueous dispersions.

Our general interpretation of the behavior of the copolymer particles at elevated temperatures is based on the volume in the cores that is not occupied by hydrophobic anchors. Let us consider the cores of the particles in which DDGG sequences are gathered. Assuming a spherical shape, the radii of the cores could be estimated using literature data of the volumes of the component groups[52] and experimental data for the degrees of polymerization of poly(DDGG) blocks and the particle aggregation numbers. A striking result from the calculations is that the theoretical radii of the cores are severalfold lower than the radii experimentally observed by cryo-TEM. This implies that there is space in the cores that is not occupied by the hydrophobic anchors and is in agreement with the assumption of the presence of PEG domains in the cores. Cryo-TEM is not a quantitative method, but approximate values of the core radii could be estimated by averaging the radii of a large number of particles in the observation area. In our case, because of the low concentration ranges studied, such estimations were not possible: several preparations were needed to shot just one object. Therefore, no size distribution data were extrated from the micrographs. Although quite uncertain, the dimensions of the aggregates shown in Figure 14 are in good agreement with the results from DLS. The following example may be given in order to demonstrate the consistency of the experimental results and the theoretical predictions. With PEG moieties of the same degree of polymerization, the polymers $(didodecyl)_2$PEG20K and $(DDGG)_{3.6}(EO)_{454}(DDGG)_{3.6}$ form aggregates with practically equal hydrodynamic radii (Table 3). However, it is immediately seen from the micrographs shown in Figure 14 that the objects are of different size being bigger for $(DDGG)_{3.6}(EO)_{454}(DDGG)_{3.6}$. This implies that the corona thickness of $(didodecyl)_2$PEG20K aggregates given by the difference between the hydrodynamic radii from DLS and the radii of the cores from cryo-TEM is higher than that of $(DDGG)_{3.6}(EO)_{454}(DDGG)_{3.6}$. A number of scaling models for polymers grafted on either planar[53,54] or curved spherical[55−57] surfaces have been developed. In both cases the thickness of the grafted layer has been found to scale as $N\sigma^{1/3}$, where N is the number of the monomer units and σ is the fraction of the surface sites grafted. With σ being 1 and 0.28 (=1/3.6) for $(didodecyl)_2$PEG20K and $(DDGG)_{3.6}(EO)_{454}(DDGG)_{3.6}$, respectively, and the same N, the corona thickness of the former is predicted to be higher than that of the latter. On the other hand, there is an energy stored in the grafted polymer chains which increases also with the molecular weight and the grafting density.[58] The stored energy is expressed in the lateral pressure between the chains. The latter has been shown to be lower for polymer chains grafted on a curved surface than the polymer on planar surfaces. Since the lateral pressure between the chains is higher for $(didodecyl)_2$PEG20K than for $(DDGG)_{3.6}(EO)_{454}(DDGG)_{3.6}$, the former polymer is expected to form aggregates with smaller core radii than $(DDGG)_{3.6}(EO)_{454}(DDGG)_{3.6}$. In summary, the expectations of higher surface curvature, i.e., smaller core radii, and higher corona thickness for $(didodecyl)_2$PEG20K compared to $(DDGG)_{3.6}(EO)_{454}(DDGG)_{3.6}$ were experimentally confirmed.

We now go back to the mechanism of the temperature-induced shrinkage of the particles. From the results and the data analysis a picture of cores consisting of lipid−mimetic anchors in which PEG−water domains are randomly distributed can be deduced. The suggested structure is quite similar to the "water in oil in water" emulsions. The results from the present study support only indirectly this model. However, recent preliminary experiments unambiguously proved the existence of aqueous compartments in which a hydrophilic dye, 5(6)-carboxyfluorescein, was successfully entrapped: the dye leaked out slowly with time from the aqueous compartments, and upon a surfactant addition the aggregates were destroyed and all 5(6)-carboxyfluorescein was released. A detailed study including dye leakage assays, SANS, and cryo-TEM is under way, and the results will be published in the near future. At elevated temperatures the PEG−water domains contain smaller amounts of water due to the well-known dehydration of PEO.[48−51] They reduce their volume which results in a decrease of the core radius, and thus particles of a higher curvature are formed. The rearrangement to a higher surface curvature is beneficial since it gives relaxation

of the lateral pressure in the coronae. Additionally, the latter become also less solvated and consequently of a lower thickness as shown for the commercially available Pluronics,[59,60] which also contributes to the decrease of the overall particle radius.

Conclusions

Self-assembly in water of a number of diblock and triblock copolymers of EO and DDGG, a monomer bearing a lipid−mimetic moiety, was investigated by a combination of static and dynamic LS as well as cryo-TEM. In the dilute region, a picture of isolated core/corona spherical particles can be derived from the data. The particle cores consist of poly(DDGG) moieties in which PEG−water domains are distributed whereas the coronae are built only of PEG chains in a brush or looping conformation for the diblock and triblock copolymers, respectively. The particles were nanoscale in size, reaching weight-average molecular weights and aggregation numbers up to 40×10^6 g/mol and 3.6×10^3, respectively. R_g/R_h ratios, calculated from the combined SLS and DLS data, were typical for micelles, being somewhat lower for the triblock copolymers. The reason for the observed shrinking of the particles at elevated temperatures is most probably due to the dehydration of the PEG chains leading to a decrease of both core radius and corona thickness.

Acknowledgment. We thank G. Karlsson for helping us with the electron microscopy studies and W. Brown for stimulating discussions. The synthetic part of the study was supported by the Bulgarian National Fund "Scientific Research" (project X-808). Financial support from the Swedish Technical Research Council is gratefully acknowledged.

References and Notes

(1) Allen, T. M.; Ryan, J. L.; Papahadjopoulos, D. *Biochim. Biophys. Acta* **1985**, *818*, 205.
(2) Allen, T. M.; Chonn, A. *FEBS Lett.* **1987**, *223*, 42.
(3) Haga, V.; Kato, F.; Yoshida, M.; Kohara, F.; Kato, Y. *Chem. Pharm. Bull.* **1986**, *34*, 2979.
(4) Hwang, K. J.; Beaumier, P. L. In *Liposomes as Drug Carriers*; Gregoriadis, G., Ed.; John Wiley & Sons: New York, 1988; pp 19−35.
(5) Allen, T. M.; Hansen, C.; Rutledge, J. *Biochim. Biophys. Acta* **1989**, *981*, 27.
(6) Needham, D.; Hristova, K.; McIntosh, T.; Dewhirst, M.; Wu, N.; Lasic, D. *J. Liposome Res.* **1992**, *2*, 411.
(7) Williams, S.; Alosco, T.; Mayhew, E.; Lasic, D.; Blankert, R. *Cancer Res.* **1993**, *53*, 3964.
(8) Uster, P. S.; Allen, T. M.; Daniel, B. E.; Mendez, C. J.; Newman, M. S.; Zhu, G. Z. *FEBS Lett.* **1996**, *386*, 243.
(9) Allen, T. M. *Curr. Opin. Colloid Interface Sci.* **1996**, *1*, 645.
(10) Johnsson, M.; Bergstrand, N.; Edwards, K. *J. Liposome Res.* **1999**, *9*, 53.
(11) Allen, T. M.; Hansen, C. B.; Lopes-de-Menezes, D. E. *Adv. Drug. Del. Rev.* **1995**, *16*, 267.
(12) Woodle, M. *Adv. Drug. Del. Rev.* **1995**, *16*, 249.
(13) Blume, G.; Cevc, G. *Biochim. Biophys. Acta* **1990**, *1029*, 91.
(14) Blume, G.; Cevc, G. *Biochim. Biophys. Acta* **1993**, *1146*, 157.
(15) Klibanov, A.; Maruyama, K.; Torchilin, V. P.; Huang, L. *FEBS Lett.* **1990**, *268*, 235.
(16) Klibanov, A.; Maruyama, K.; Beckerleg, A. M.; Torchilin, V. P.; Huang, L. *Biochim. Biophys. Acta* **1991**, *1062*, 142.
(17) Allen, T. M.; Hansen, C.; Martin, F.; Redemann, C.; Yau-Young, A. *Biochim. Biophys. Acta* **1991**, *1066*, 29.
(18) Allen, T. M.; Hansen, C. *Biochim. Biophys. Acta* **1991**, *1068*, 133.
(19) Mayhew, E.; Lasic, D.; Babbar, S.; Martin, F. *Int. J. Cancer* **1992**, *51*, 302.
(20) Chonn, A.; Cullis, P. R. *Curr. Opin. Biotechnol.* **1995**, *6*, 698.
(21) Lasic, D.; Martin, F. *Stealth Liposomes*; CRC Press: Boca Raton, FL, 1995.
(22) Rangelov, S.; Petrova, E.; Berlinova, I.; Tsvetanov, Ch. *Polymer* **2001**, *42*, 4483.
(23) Rangelov, S.; Tsvetanov, Ch. *Des. Monomers Polym.* **2001**, *4*, 39.
(24) Rangelov, S.; Tsvetanov, Ch. *Polym. Bull. (Berlin)* **2001**, *46*, 471.
(25) Rangelov, S.; Brown, W. *Polymer* **2000**, *41*, 4825.
(26) Chu, B. *Laser Light Scattering, 2;* Academic Press: New York, 1991.
(27) Jakes, J. *Czech. J. Phys. B* **1988**, *38*, 1305.
(28) Kenworthy, A.; Simon, S. A.; McIntosh, T. J. *Biophys. J.* **1995**, *68*, 1903.
(29) Edwards, K.; Johnsson, M.; Karlsson, G.; Silvander, M. *Biophys. J.* **1997**, *73*, 258.
(30) Johnsson, M.; Hansson, P.; Edwards, K. *J. Phys. Chem. B* **2001**, *105*, 8420.
(31) Sou, K.; Endo, T.; Takeoka, S.; Tsushida, E. *Bioconjugate Chem.* **2000**, *11*, 372.
(32) Lasic, D. D.; Woodle, M. C.; Martin, F. J.; Valentincic, T. *Period. Biol.* **1991**, *93*, 287.
(33) Burchard, W. *Adv. Polym. Sci.* **1983**, *48*, 1.
(34) Thurn, A.; Burchard, W.; Niki, R. *Colloid Polym. Sci.* **1987**, *265*, 653.
(35) Devanand, K.; Selser, J. C. *Macromolecules* **1991**, *24*, 5943.
(36) Alami, E.; Almgren, M.; Brown, W. *Macromolecules* **1996**, *29*, 2229.
(37) Rangelov, S.; Almgren, M.; Tsvetanov, Ch.; Edwards, K. *Macromolecules*, in press.
(38) Seery, T.; Yassini, M.; Hogen-Esch, T.; Amis, E. *Macromolecules* **1992**, *25*, 4784.
(39) Fujiwara, T.; Miyamoto, M.; Kimura, Y. *Macromolecules* **2000**, *33*, 2782.
(40) Fujiwara, T.; Miyamoto, M.; Kimura, Y.; Iwata, T.; Doi, Y. *Macromolecules* **2001**, *34*, 4043.
(41) Bockstaller, M.; Kohler, W.; Wegner, G.; Fytas, G. *Macromolecules* **2001**, *34*, 6353.
(42) Cao, L.; Manners, I.; Winnik, M. *Macromolecules* **2001**, *34*, 3353.
(43) Lin, F.; Lin, G. *Macromolecules* **2001**, *34*, 1302.
(44) Butun, V.; Armes, S.; Billingham, N. C.; Tuzar, Z.; Rankin, A.; Eastoe, J.; Heenan, R. K. *Macromolecules* **2001**, *34*, 1503.
(45) McConnell, G. A.; Gast, A. P.; Huang, J. S.; Smith, S. D. *Phys. Rev. Lett.* **1993**, *71*, 2102.
(46) McConnell, G. A.; Lin, E. K.; Gast, A. P.; Huang, J. S.; Lin, M. Y.; Smith, S. D. *Faraday Discuss.* **1994**, *98*, 121.
(47) Gast, A. P. *Langmuir* **1996**, *12*, 4060.
(48) Bailey, F. E.; Koliske, J. V. *Alkylene Oxides and Their Polymers*; Marcel Dekker: New York, 1991.
(49) Saeki, S.; Kuwahara, N.; Nakata, M.; Kaneko, M. *Polymer* **1975**, *17*, 685.
(50) Kjellander, R.; Florin, E. *J. Chem. Soc., Faraday Trans.* **1981**, *1*, 2053.
(51) Matsuyama, A.; Tanaka, F. *Phys. Rev. Lett.* **1990**, *65*, 341.
(52) Nagle, J. F.; Tristram-Nagle, S. *Biochim. Biophys. Acta* **2000**, *1469*, 159.
(53) Alexander, S. *J. Phys. (Paris)* **1977**, *38*, 983.
(54) de Gennes, P. G. *Macromolecules* **1980**, *13*, 1069.
(55) Daoud, M.; Cotton, J. P. *J. Phys. (Paris)* **1982**, *43*, 531.
(56) d'Oliveira, J. M. R.; Martinho, J. M. G.; Xu, R.; Winnik, M. A. *Macromolecules* **1995**, *28*, 4750.
(57) Vagberg, L. G. M.; Cogan, K. A.; Gast, A. P. *Macromolecules* **1991**, *24*, 1670.
(58) Milner, S.; Witten, T.; Cates, M. *Macromolecules* **1988**, *21*, 2610.
(59) Almgren, M.; Brown, W.; Hvidt, S. *Colloid Polym. Sci.* **1995**, *273*, 2.
(60) Yang, L.; Alexandridis, P.; Steytler, D.; Kositza, M.; Holzwarth, J. *Langmuir* **2000**, *16*, 8555.

MA012246+